# Dynamic localization of Lyapunov vectors in spacetime chaos

Arkady Pikovsky† and Antonio Politi‡

† Department of Physics, University of Potsdam, Am Neuen Palais, PF 601553, D-14415, Potsdam, Germany

<sup>‡</sup> Istituto Nazionale di Ottica, Largo E Fermi 6, Firenze-Arcetri, I-50125, Italy

Received 6 October 1997 Recommended by P Grassberger

**Abstract.** We study the dynamics of Lyapunov vectors in various models of one-dimensional distributed systems with spacetime chaos. We demonstrate that the vector corresponding to the maximum exponent is always localized and the localization region wanders irregularly. This localization is explained by interpreting the logarithm of the Lyapunov vector as a roughening interface. We show that for many systems, the 'interface' belongs to the Kardar–Parisi–Zhang universality class. Accordingly, we discuss the scaling behaviour of finite-size effects and self-averaging properties of the Lyapunov exponents.

PACS number: 0545

#### 1. Introduction

Sensitive dependence on initial conditions is an intrinsic and probably the most important property of chaotic motion [1, 2]. This sensitivity is quantified by the largest Lyapunov exponent, which, roughly speaking, represents the average exponential growth rate of initially small perturbations. In numerical studies, the usual procedure involves the simultaneous solution of the nonlinear equations and of the linearized equations for a perturbation (usually referred to as the Lyapunov vector); the Lyapunov exponent is thus obtained from the exponential growth rate of the perturbation amplitude. Although this method can rarely be implemented in real experiments, there are ways to estimate the Lyapunov exponent from the observed process, provided that enough data is available for reconstructing the local dynamics [3].

The extension of the notion of Lyapunov exponent to spacetime chaos is not straightforward. Indeed, in a system with a few degrees of freedom, it is essentially not important what initial conditions are chosen for the Lyapunov vector as, after an initial transient, the component with the maximal growth rate dominates for almost all initial choices. This may not be true in a distributed, infinitely extended system, since the transient time can be, formally, infinite. For instance, if one considers a perturbation initially localized in space, the spreading process becomes an important feature that leads to the notion of velocity-dependent or localized Lyapunov exponents [4, 5]. Intrinsically close to this is the notion of generalized Lyapunov exponents [6], where the linear perturbation is assumed to have an exponential (on average) spatial profile. From the other side, if the initial Lyapunov vector is homogeneous in space, one can expect this homogeneity to be conserved at least

in a statistical sense during the evolution in time. The computation of Lyapunov exponents with such a type of vectors appears to be the closest analogue to the procedure adopted for systems with a finite number of degrees of freedom.

In any case, the main difference connected to distributed systems is the existence of a second limit (the so-called thermodynamic limit, corresponding to the system size L tending to infinity) that must be taken together with the usual limit  $T \to \infty$ , where T is the observation time, required by the very definition of the Lyapunov exponent. As any simulation is performed on a finite system for a finite time, it is important to investigate the convergence properties of the two limits. This is particularly relevant to provide a rigorous basis for an accurate determination of the Lyapunov exponents in extended systems. In fact, the Lyapunov exponents are usually determined by employing only qualitative criteria to fix the system size and the number of iterations (if the limits are not imposed by the computing facilities, as it is often the case). In particular, it is useful to find the optimal iteration time  $T_0$  for a fixed L and thereby determine the finite-size corrections to increase the accuracy of the estimated Lyapunov exponents.

In this paper, we consider several dynamical systems ranging from lattices of logistic and symplectic maps, to partial differential equations, and even differential-delay equations. In all cases, we look at the behaviour of the maximum Lyapunov exponent and of the corresponding Lyapunov vector for fixed size L, and increasing time T. We then study how the instability properties depend on L. This is done by considering the Lyapunov vectors as spatially statistically homogeneous objects (of course, the underlying spacetime chaos is assumed to be statistically homogeneous in space and time) and investigate their statistical properties. More precisely, we introduce a single real variable to characterize the perturbation size in any spatial point, even when the number of local variables is larger than one (as for some models—see the examples in section 2 below). Since the statistical properties depend on L, these dependencies can be described as finite-size effects in a by now standard way in statistical mechanics [7].

The starting point is the qualitative observation that the Lyapunov vector is highly localized in space (cf [8–13]). In section 2, we demonstrate that this holds for all the different models. The more detailed analysis performed in section 3 also demonstrates quantitatively that the statistical properties of the Lyapunov vectors are the same for the various models, thus allowing us to speak of a universal scenario. The key element for understanding this universality is the interpretation of the *logarithm* of the local amplitude of the perturbation as a rough drifting surface. By applying the ideas of the theory of roughening interfaces [14, 15], in section 3 we demonstrate that the Lyapunov vectors belong to the universality class of the Kardar–Parisi–Zhang (KPZ) equation [16]. This analogy allows us to interpret the Lyapunov exponent as the average velocity of the interface and to predict finite-size corrections that are actually compared with the simulations in section 5. One important implication of the localization of Lyapunov vectors is the dependence of the fluctuations of the Lyapunov exponent on the vector norm; in section 4, we show that one can choose a norm that minimizes the fluctuations.

### 2. Lyapunov vectors in spacetime chaos: observations

Localization of the Lyapunov vectors corresponding to all Lyapunov exponents has been noticed and discussed in some distributed systems and suitable localization lengths have been introduced to quantify the amount of localization of the various vectors [8–12]. As the nature of the localization is not yet theoretically clear, we prefer to start from numerical observations, illustrating the properties of the Lyapunov vectors in several models

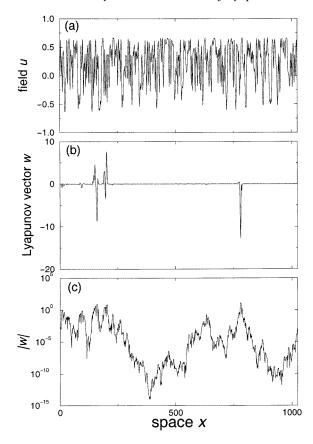


**Figure 1.** (a) The field u in coupled logistic maps (L=1024); (b) the instantaneous profile of the corresponding Lyapunov vector at the same time as u; (c) the profile of the Lyapunov vector in the logarithmic scale.

of spacetime chaos. In all models (except for the differential-delay equation, where it is not necessary), periodic boundary conditions are assumed. As the perturbation grows exponentially in time, we always refer to the normalized vector (the norm being set equal to the system length in some given units).

# 2.1. Coupled logistic maps

A popular discrete-time, discrete-space model of diffusively coupled logistic maps has the form

$$u(t+1,x) = (1-2\varepsilon)f(u(t,x)) + \varepsilon(f(u(t,x-1)) + f(u(t,x+1))),$$
  
  $x = 1, \dots, L.$  (1)

Here f(u) = 4u(1-u) is the logistic map in the regime of fully developed chaos, while the parameter  $\varepsilon$  describes the coupling. To obtain the equation for the Lyapunov vector w(t, x), we have to linearize (1), obtaining

$$\begin{split} \tilde{w}(t,x) &\equiv f'(u(t,x))w(t,x) \\ w(t+1,x) &= (1-2\varepsilon)\tilde{w}(t,x) + \varepsilon(\tilde{w}(t,x-1) + \tilde{w}(t,x+1)). \end{split} \tag{2}$$

Below, we consider only the case of 'democratic' coupling  $\varepsilon = \frac{1}{3}$ . The Lyapunov vector is generated by iterating simultaneously (1) and (2). After a sufficiently long transient, the field u is a homogeneous random process as seen in figure 1(a), while w has the typical

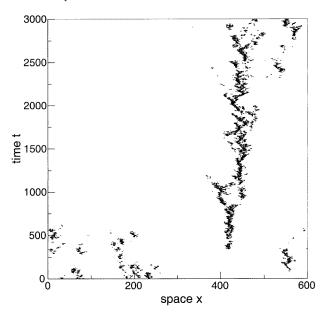


**Figure 2.** The spatio-temporal diagram of the evolution of the Lyapunov vector in model (2). The sites where the amplitude of the vector |w| exceeds a threshold are marked black.

shape reported in figure 1. One immediately notices (see figure 1(b)) that the Lyapunov vector is essentially different from zero only in small spatial domains. To demonstrate that the localization is a persistent property of the Lyapunov vector, we depict a spacetime diagram in figure 2. There, one can see that the localization region is slowly wandering, and different spikes of the field can appear and disappear. We call this behaviour dynamical localization, in contrast to the static localization of wavefunctions in one-dimensional disordered potentials (Anderson localization).

In order to see whether the above features are typical of spacetime chaos, below we follow the evolution of Lyapunov vectors in models of different nature.

### 2.2. Coupled symplectic maps

In contrast to the dissipative system of coupled logistic maps, models of coupled symplectic maps preserve the Hamiltonian structure (in particular, phase volumes are conserved). We consider here coupled standard maps [17, 18],

$$I(t+1, x) = I(t, x) + K \sin(\theta(t, x)) + \alpha \sin(\theta(t, x) - \theta(t, x - 1)) + \alpha \sin(\theta(t, x) - \theta(t, x + 1))\theta(t+1, x) = \theta(t, x) + I(t+1, x),$$

where both variables I and  $\theta$  are assumed to be  $2\pi$ -periodic. In this case, the infinitesimal perturbation is characterized by the two variables  $\delta I(t,x)$  and  $\delta \theta(t,x)$  which satisfy the recursive relation obtained by linearizing the above equation.

It is natural to define the Lyapunov vector in terms of the local norm,

$$w_{sm}(t,x) = \sqrt{[\delta I(t,x)]^2 + [\delta \theta(t,x)]^2}.$$

The spatial profile of  $w_{sm}$  is shown in figure 3(a).

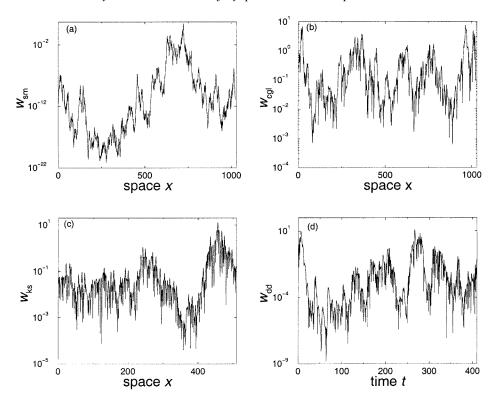


**Figure 3.** The Lyapunov vectors for different models described in the text: (a) coupled symplectic maps with K = 5,  $\alpha = 1$ , L = 1024; (b) the complex Ginzburg-Landau equation with  $c_1 = -2$ ,  $c_3 = 2$ , L = 1024; (c) Kuramoto-Sivashinsky equation with L = 512; (d) Ikeda differential-delay equation with a = 5,  $\tau = 409.6$ .

# 2.3. Partial differential equations

We consider here two models that are widely used in studies of spacetime chaos. The first is the complex Ginzburg-Landau equation [19]

$$\frac{\partial a}{\partial t} = a + (1 + ic_1) \frac{\partial^2 a}{\partial x^2} - (1 + ic_3)|a|^2 a,\tag{3}$$

which describes the evolution of a complex field a(t, x) in a region  $0 \le x \le L$ . The linear perturbation field  $\delta a$  is also complex, and the Lyapunov vector is constructed by taking the absolute value

$$w_{cgl}(t, x) = |\delta a(t, x)|$$

(see figure 3(b) for a snapshot of the Lyapunov vector).

Another partial differential equation model we present here is the Kuramoto–Sivashinsky equation for a real field u(t, x) [20]

$$\frac{\partial u}{\partial t} + uu_x + u_{xx} + u_{xxxx} = 0. (4)$$

The linear perturbation field  $\delta u(t, x)$  is also real; its absolute value,  $w_{ks} = |\delta u(t, x)|$ , is shown in figure 3(c).

## 2.4. Differential-delay equation

As it has been shown in [21], a differential-delay equation of the form

$$\frac{\mathrm{d}u}{\mathrm{d}t} = F(u(t), u(t-\tau)),$$

can be considered as a spatially extended system with an effective 'length'  $L=\tau$  and effective time measured in number of delay units. Thus, a piece of the linear perturbation field  $\delta u(t)$  of length  $\tau$  represents a characteristic spatial profile. As a concrete example, we consider here the Ikeda model

$$\frac{\mathrm{d}u}{\mathrm{d}t} = -u + a\sin u(t - \tau),$$

describing the dynamics of a passive nonlinear optical resonator [22]. Investigation of this model is also instructive, since it furnishes evidence of localization in a system with 'spatially' asymmetric coupling. The asymmetry here is a straightforward consequence of the temporal asymmetry; its main consequence is the directed propagation of the localization regions in addition to the above-mentioned irregular wandering. A snapshot of the Lyapunov vector  $w_{dd} = |\delta u(t)|$  is shown in figure 3(d).

Altogether, the data in figure 3 gives numerical evidence that the Lyapunov vector is dynamically localized if the system size is large enough. In all models, the localization is made transparent by representing the perturbation amplitude in a logarithmic scale.

### 3. Lyapunov vectors as roughening interfaces

The main idea for a quantitative description of dynamical localization of Lyapunov vectors comes from the analogy with the dynamics of rough interfaces. For the particular case of coupled skewed Bernoulli maps, such an analogy has been suggested by a suitable transformation of the equation for w and numerically confirmed by the simulations [10]. Below, we demonstrate that this analogy is much more general, applying to all the above-described models, so that they appear to belong to the same universality class described by the KPZ equation.

The first step consists of passing from the vector field to the logarithm of its absolute value. In this way, the field in figure 1(b) is transformed into the profile shown in figure 1(c). In the following, we shall interchangeably refer to

$$h(t, x) = \log|w(t, x)| \tag{5}$$

as to either the profile or the 'interface'. The dynamics of the Lyapunov vector is characterized by two main features: an exponential growth and irregular fluctuations. The former corresponds to a linear movement of the profile, thus implying that the Lyapunov exponent is nothing but the interface velocity. The latter is a manifestation of the roughening process: if we start from a flat profile (meaning that the initial condition for the linearized equations is spatially uniform), the width of the interface grows in time, saturating to a value that diverges for increasing the system size. This is precisely what is observed in numerical experiments, and explains qualitatively the dynamical localization: the observed Lyapunov vector is the exponential of the roughened interface so that only a small region near the maximum can be seen as in figures 1(b) and 2.

One rather technical remark is in order. Defining the interface with (5), we get logarithmic singularities at the zeros of the Lyapunov vector w. Such zeros can be quite rare for discrete mappings and whenever the amplitude of the Lyapunov vector is defined as a local norm of a multicomponent field (like for the complex Ginzburg–Landau equation). In

the case of one-component continuous-space field (as, e.g. the above-mentioned Kuramoto–Sivashinsky and differential-delay equations), they are unavoidable, as the Lyapunov vector changes sign. One way to avoid this difficulty is by introducing a local averaging of the Lyapunov vector at small scales, i.e. by replacing |w(x)| by

$$|w_{\epsilon}(x)| = \frac{1}{\epsilon} \int_{-\epsilon/2}^{\epsilon/2} \mathrm{d}x \, |w(x)|.$$

However, even without this trick, no real numerical problems arise, as the singularities are very weak (one can check that logarithmic singularities give a minor contribution to the statistical characteristics of the interface such as its width and mean position) and since continuous (in space) systems are discretized any way.

To proceed to a quantitative description, we compare the properties of the Lyapunov vectors with those predicted by the models of roughening interfaces. The proper candidate is the KPZ equation, since it applies to the phenomenologically relevant case of a linear diffusive process with multiplicative noise

$$\frac{\partial w}{\partial t} = \xi(t, x)w + \frac{\partial^2 w}{\partial x^2},\tag{6}$$

where  $\xi(t, x)$  mimics a fluctuating local amplification of perturbation, while the second-order derivative accounts for the spatial coupling. The Hopf–Cole transformation,  $h = \log w$ , leads to

$$\frac{\partial h}{\partial t} = h_{xx} + h_x^2 + \xi(t, x),\tag{7}$$

which is the KPZ equation in its standard form [14-16].

It is not possible to derive exactly equation (6), starting from the models described in the previous section. Thus, the only way to verify that the KPZ equation is a good model for the Lyapunov vector is by checking that the predictions of the KPZ equation are consistent with the characteristics of the observed dynamics. The essential part of these predictions can be formulated in the form of scaling relations for the time and space dependencies of the relevant indicators. Verifying these scalings will allow us to conclude that the models above belong to the KPZ universality class.

In the statistically stationary regime, the local slopes  $\nabla h$  are uncorrelated and their distribution is Gaussian, so that the spatial profile can be seen as a Brownian motion [14, 15]. Thus, the average saturated interface-width  $W(t = \infty)$ , defined from

$$W^2(\infty) = \langle (h - \langle h \rangle)^2 \rangle,$$

scales with the system length L as

$$W(\infty) \sim L^{1/2}.\tag{8}$$

By introducing the spatial power spectrum S(k) of the field h(x), the above scaling relation can be reformulated as,

$$S(k) \sim k^{-2} \tag{9}$$

which is, correspondingly, expected to hold in the region of small wavenumbers  $k \to 0$ .

For the temporal scaling, the theory predicts that the interface width asymptotically grows as

$$W^2(t) \sim t^{\beta} \tag{10}$$

with  $\beta = \frac{2}{3}$ , provided that the interface is initially flat and the system size is large enough to ensure that the saturation phenomena described by equation (8) are still negligible for



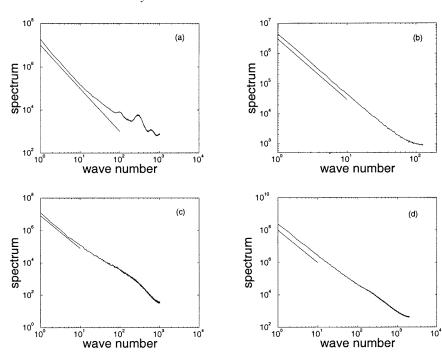


**Figure 4.** The spatial spectra of the 'interfaces' for the models described in the text (with the same parameters as in figure 3): (a) the Kuramoto–Sivashinsky equation (L=1024); (b) the coupled standard maps (L=256); (c) the complex Ginzburg–Landau equation (L=1024); (d) the differential-delay Ikeda model  $(\tau=409.6)$ . The straight lines have slope -2.

these times. Both relations (9) and (10) have been checked numerically for the above-described models. The results for the spatial spectrum (9) are presented in figure 4. One can see that relation (9) is very well satisfied in all models. This is the first confirmation that the interpretation of the logarithm of the Lyapunov vector as an interface makes sense. However, the above agreement cannot still be taken as conclusive. In fact, the same spatial dependence as in KPZ is shared by the Edwards–Wilkinson equation [23] (a linear equation obtained by dropping the quadratic term in KPZ equation).

Aiming at a correct identification of a proper model for the Lyapunov-vector dynamics, the test of relation (10) is more informative since we know that, at variance with KPZ,  $\beta = \frac{1}{2}$  in the Edwards–Wilkinson model. As it can be seen from figure 5, the numerical test of the temporal behaviour gives less definite results. However, a slower-than-expected growth rate is a frequent feature affecting the dynamics of roughening interfaces [14, 15] and can be attributed to the weakness of the effective nonlinearity. In fact, the nonlinear exponent  $\frac{2}{3}$  can be unambiguously observed only in systems sufficiently large to ensure that the width W does not saturate before the nonlinear effects become visible. For the models considered here, we can proceed to very large sizes only for lattice systems, since the required computation time becomes enormously large in the partial differential equations. Nevertheless, in all models there is a clear tendency, over the accessible timescales, for the time exponent to exceed the linear value  $\frac{1}{2}$  even if  $\frac{2}{3}$  is not still attained.

It is worth noting that the nonlinearity in the KPZ equation has a clear physical meaning for the Lyapunov vectors. It is connected to the fact that the propagation velocity of a tilted interface is different from that of a non-tilted one. For the Lyapunov vector, the tilt of the

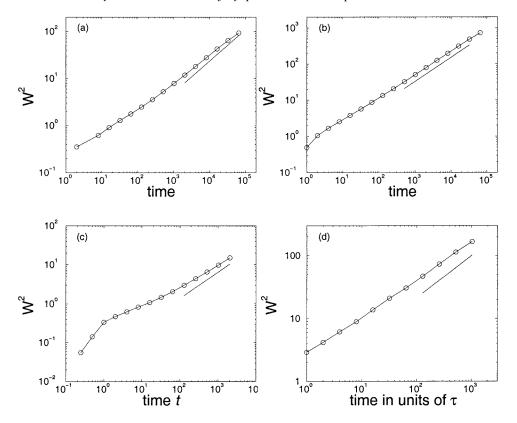


**Figure 5.** The 'interfaces' width growth for (a) the coupled logistic maps (L=8192), (b) the coupled standard maps (L=8192), (c) the complex Ginzburg–Landau equation (L=4096), and (d) the differential-delay Ikeda model  $(\tau=2000)$ . The straight lines have the slope  $\frac{2}{3}$  predicted by KPZ theory.

logarithm means that the vector itself has a spatially exponential profile. This notion is at the basis of the definition of the generalized Lyapunov exponent according to [6].

The results presented above show that there is a large class of models of spacetime chaos for which the Lyapunov vectors belong to the KPZ universality class. We want to emphasize, however, that not all systems have this property. First, there are cases in which the effective noise in the dynamics of the Lyapunov vector vanishes, e.g. a lattice of Bernoulli maps. A less special class of models is represented by some continuous-time Hamiltonian systems (the Fermi–Pasta–Ulam model and some similar lattices of nonlinear oscillators) where the localization properties differ significantly from the predictions of the KPZ theory. These systems are currently a subject of special investigation.

## 4. Self-averaging of Lyapunov exponents

The Lyapunov exponent of a chaotic system is defined as a time-averaged quantity. One can also define finite-time exponents, which are distributed in a certain interval and converge to the Lyapunov exponent as the finite time interval tends to infinity [24, 25]. Roughly speaking, finite-time exponents measure the fluctuations of the growth rate. A natural question arises: How do these fluctuations depend on the system size in a distributed

system? If the fluctuations decrease with the system size, one can speak of self-averaging of the Lyapunov exponent.

In order to compute the Lyapunov exponent, one needs to define a norm of the Lyapunov vector. In the following we shall find that it is convenient to introduce the generalized q-norm  $(0 \le q < \infty)$  according to

$$N_q(t) = \left[\frac{1}{L} \int_0^L |w(t, x)|^q \, \mathrm{d}x\right]^{1/q}.$$
 (11)

This norm can be rewritten by referring to the interface profile as

$$N_q(t) = \left[ \frac{1}{L} \int_0^L e^{qh(t,x)} dx \right]^{1/q}.$$
 (12)

The norm commonly used in numerical calculations is the Euclidean one (q = 2). For future considerations, it is important to notice that the 0-norm is nothing else than the exponent of the average position of the interface h(x),

$$N_0(t) = \lim_{q \to 0} N_q = \exp\left[\frac{1}{L} \int_0^L h(t, x) \, \mathrm{d}x\right]$$

while the ∞-norm corresponds to the maximum of the perturbation field

$$N_{\infty} = |w_{\text{max}}| = e^{h_{\text{max}}}$$
.

In all cases we have considered, the difference between the 'highest' and the 'lowest' point in the interface remains finite in finite systems. This result is not surprising, since the spatial coupling prevents an indefinite growth of the local derivative. Notice that the same is also true for inhomogeneous configurations generated by juxtaposing two regions characterized by different chaotic properties: in such a case, the perturbation grows with different velocities in the two regions, but propagation phenomena are eventually responsible for homogenizing the evolution. Accordingly, the Lyapunov exponent

$$\lambda = \lim_{T \to \infty} \frac{\log N_q(T) - \log N_q(0)}{T}$$

is independent of the q-norm adopted. This is a standard result in low-dimensional chaos, but is much less obvious in distributed systems. However, when considering the finite-time Lyapunov exponent

$$\lambda_q(T) = \frac{\log N_q(T) - \log N_q(0)}{T}$$

the difference between the various q-norms can be important as we argue below. We have shown that the interface h(t,x) can be considered as a roughening field belonging to the KPZ universality class. This means that the fluctuations of the interface position have a finite correlation length  $\ell_c$ . Thus, in calculating the 0-norm, i.e. the mean interface position, we sum many,  $L/\ell_c$ , uncorrelated contributions. Accordingly, as the system length L grows, the fluctuations of the interface position decrease as  $L^{-1/2}$ . In the opposite limit, only one point (the maximum) contributes to the  $\infty$ -norm; its fluctuations, in turn, do not depend at all on the system length. Summarizing, we expect that the dependence of the fluctuations of the finite-time Lyapunov exponent on the system size is different for different norms and the least fluctuating is the 0-norm. In figure 6, we present numerical results for the variance of the finite-time Lyapunov exponent for different norms and different system lengths. The calculations are in full agreement with the previous theoretical estimations. They show that the Lyapunov exponent can be considered as a self-averaging quantity only if the 0-norm

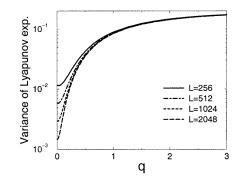


**Figure 6.** Fluctuations of instantaneous Lyapunov exponents in a lattice of L coupled logistic maps, as a function of the norm parameter q.

is used. However, it is important to notice that the lack of fluctuations for the finite-time estimate does not imply that the limit  $T \to \infty$  is not necessary. In the next section we discuss precisely the role of finite-size corrections.

#### 5. Finite-size corrections

The dynamics of the Lyapunov vector has characteristic spatial and temporal scales that must be taken into account in the calculation of the Lyapunov exponent. Consider a system of size L, and take a uniform initial condition for the linear perturbation. Let us define the time-T Lyapunov exponent with reference to the 0-norm as

$$\lambda(T, L) = \left\langle \frac{\log N_0(T) - \log N_0(0)}{T} \right\rangle,\tag{13}$$

where the angular brackets denote the ensemble average being introduced to omit fluctuations (the usual Lyapunov exponent is  $\lambda(\infty, L)$ ). According to the theory of KPZ dynamics [15], the following scaling relation holds

$$\lambda(T, L) - \lambda_{\infty} = L^{-1} f(TL^{-3/2}). \tag{14}$$

Here  $\lambda_{\infty} = \lambda(\infty, \infty)$  is the largest Lyapunov exponent for an infinite system and f(y) is a scaling function that approaches a constant for large y and scales as  $y^{-2/3}$  for small y. This general relation has several consequences. First, it gives the scaling of the largest Lyapunov exponent with the system length,

$$\lambda(\infty, L) - \lambda_{\infty} \sim L^{-1}$$
.

This is the first important result that could be used to remove finite-size corrections, improving the accuracy of the Lyapunov exponent calculations.

Moreover, still for a system of a given size L, we can estimate the transient time needed for the statistically stationary regime to be established (i.e. for the roughened interface to be fully developed) as

$$T_{tr} \sim L^{3/2}$$
. (15)

For short times and large system size, we get from equation (14)

$$\lambda(T,\infty) - \lambda_{\infty} \sim T^{-2/3}. (16)$$

This relation provides an alternative way to estimate the asymptotic Lyapunov exponent by plotting  $\lambda(T, L)$  versus  $T^{-2/3}$  for large L as it can be seen in figure 7.

Upon assuming that  $\lambda_{\infty}$  is known, one can test the universal behaviour of the corrections predicted by KPZ, by plotting the finite-time finite-size Lyapunov exponent in scaled



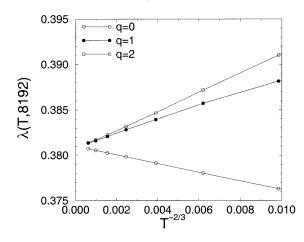


**Figure 7.** Estimating  $\lambda_{\infty}$  in coupled logistic maps, by plotting  $\lambda(T, 8192)$  versus  $T^{-2/3}$ , for different norms.

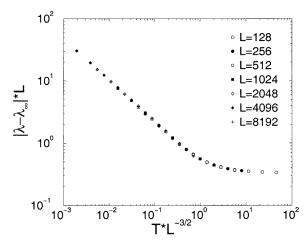


**Figure 8.** Scaling of finite-size effects in the Lyapunov exponent for coupled logistic maps.

coordinates. The choice adopted in figure 8 reveals a good data collapse confirming the validity of equation (14); the curve along which all points align is nothing but the universal function f.

Now, we have all the elements to discuss what the optimal strategy is to determine the maximum Lyapunov exponent in a distributed system. Given a system of size L, we learned that the Lyapunov exponent cannot be estimated with a better accuracy than 1/L. Since the deviation from the asymptotic result (starting with a flat profile) decreases as  $T^{-2/3}$ , it makes no sense to go beyond a time  $T_0 \approx L^{3/2}$ , which is thus the order of magnitude of the optimal time. Obviously, an estimate of the Lyapunov exponent from a single trajectory is affected by fluctuations as well as by systematic deviations. If we use the 0-norm, the statistical error is of the order of  $1/\sqrt{L}$  for each iteration and of the order of  $L^{-5/4}$  after a time  $T_0$ . Therefore, we can conclude that the statistical error is smaller than the finite-size correction and there is no need to further improve the statistics.

It is important to note that in all the estimates, the prefactors in the power-law dependencies can be important, and for a real estimation, say, of time  $T_0$ , one needs to know the prefactors at least approximately. Also dependencies of the prefactors on the system parameters may be highly nontrivial, as the effective parameters of the KPZ equation (diffusion coefficient, nonlinearity constant, noise amplitude) depend on the parameters of

the system with spacetime chaos in a complex way.

As a further consideration for an accurate determination of  $\lambda_{\infty}$ , we want to notice that in all cases we have investigated, the 1- and 2-norm yield a convergence from above, while the 0-norm leads to a convergence from below (see, for instance, figure 7). This suggests the existence of an optimal q value for which finite-size corrections automatically vanish. We leave a quantitative discussion of this point to future investigations.

#### 6. Conclusion

In this paper we have shown that in a wide class of dynamical models of spacetime chaos, the large-scale behaviour of the Lyapunov vector can be assimilated to that of a rough moving interface belonging to the KPZ universality class. Correspondingly, the finite-size scaling effects for Lyapunov exponents can be directly extracted from the theory of roughening surfaces.

It is worth discussing why so many different systems have quantitatively similar properties and why, from the other side, not all models demonstrate such a behaviour. Generally, the linear perturbation field satisfies a linear equation, where the chaotic field plays the role of a multiplicative parameter and a spatial coupling is present. Essentially, these elements are also present in the noisy diffusion equation (6) that is exactly equivalent to the KPZ equation (7). It is however important to recall that in some of the above-discussed models the interaction is not purely diffusive. The case of coupled symplectic maps is particularly instructive and deserves a separate discussion, since it belongs to the class of conservative models in which we have found examples such as, e.g. the Fermi–Pasta–Ulam lattice, of localization properties different from those reported above. The numerical results give firm evidence that the perturbation field for the lattice of symplectic maps does belong to the KPZ class, which is an essentially dissipative model. A possible explanation of the apparent paradox is that when a perturbation is followed in time, the time-reversal symmetry is broken, giving rise to dissipative-like features. All the above consideration are exemplified by the following Hamiltonian equation with multiplicative noise

$$w_{tt} - w_{xx} - \xi(t, x)w = 0.$$

The second-order derivative in time makes the problem invariant under time-reversal and implies that the second-order derivative in space gives rise to wave propagation rather than to diffusion. If we look for a growing solution, then after the substitution

$$w(t, x) = e^{\lambda t} W(t, x)$$

we obtain

$$W_{tt} + 2\lambda W_t + \lambda^2 W = W_{xx} + \xi(t, x)W.$$

If we now assume that  $\lambda$  is large and neglect the second time derivative on the l.h.s., we get a dissipative equation of type (6). However, this last step is not obvious and this may be the reason why in some conservative models the original second-order equation in time cannot yield a KPZ-like evolution.

In this paper we restricted our considerations to one-dimensional models. In one spatial dimension, the dynamics of the KPZ equation is well understood, which cannot be said in two and three dimensions. Properties of Lyapunov vectors in many-dimensional systems with spacetime chaos will be the subject of a future work. Also, we looked only at the largest Lyapunov exponent and the corresponding Lyapunov vector. As a distributed system has a whole spectrum of Lyapunov exponents, one can also pose the question of their localization properties.

## Acknowledgments

We would like to thank O Rudzick, H Chaté, P Grassberger, G Grinstein and D Shepelyansky for valuable discussions. AP acknowledges support from the Max Planck Society. This work was supported by the German–Italian VIGONI programme, the ISI Foundation (Torino) and the EU Human Capital Mobility Network ERB-CHRX-CT940546.

#### References

- [1] Ott E 1992 Chaos in Dynamical Systems (Cambridge: Cambridge University Press)
- [2] Schuster H G 1988 Deterministic Chaos, An Introduction (Weinheim: VCH)
- [3] Kantz H and Schreiber T 1997 Nonlinear Time Series Analysis (Cambridge: Cambridge University Press)
- [4] Deissler R S and Kaneko K 1987 Phys. Lett. 119A 397
- [5] Pikovsky A S 1993 Chaos 3 225
- [6] Politi A and Torcini A 1992 Chaos 2 293
- [7] Cardy J L 1988 Finite-size Scaling (Amsterdam: North-Holland)
- [8] Giacomelli G and Politi A 1991 Europhys. Lett. 15 387
- [9] Falcioni M, Marconi U M B and Vulpiani A 1991 Phys. Rev. A 44 2263
- [10] Pikovsky A S and Kurths J 1994 Phys. Rev. E 49 898
- [11] Kaneko K 1986 Physica D 23 436
- [12] Chaté H 1993 Europhys. Lett. 21 419
- [13] Lin D C 1996 Physica D 95 244
- [14] Barabási A-L and Stanley H E 1995 Fractal Concepts in Surface Growth (Cambridge: Cambridge University Press)
- [15] Halpin-Healy T and Zhang Y-C 1995 Phys. Rep. 254 215
- [16] Kardar M, Parisi G and Zhang Y C 1986 Phys. Rev. Lett. 56 889
- [17] Kaneko K and Bagley R 1985 Phys. Lett. 110A 435
- [18] Wood B P, Lichtenberg A J and Lieberman M A 1990 Phys. Rev. A 42 5885
- [19] Shraiman B I et al 1992 Physica D 57 241
- [20] Hyman J M, Nicolaenko B and Zaleski S 1986 Physica D 23 265
- [21] Giacomelli G and Politi A 1996 Phys. Rev. Lett. 76 2686
- [22] Ikeda K 1979 Opt. Commun. 30 257
- [23] Edwards S F and Wilkinson D R 1982 Proc. R. Soc. A 381 17
- [24] Eckmann J P and Procaccia I 1986 Phys. Rev. A 34 659
- [25] Crisanti A, Paladin G and Vulpiani A 1993 Products of Random Matrices in Statistical Physics (Berlin: Springer)